JOURNAL OF MATERIALS SCIENCE **38** (2003) 3729–3739

Optimization of the VARTM process for enhancement of the degree of devolatilization of polymerization by-products and solvents

M. GRUJICIC*, K. M. CHITTAJALLU
Department of Mechanical Engineering, Clemson University, Clemson, SC 29634, USA
E-mail: mica.grujicic@ces.clemson.edu

S. WALSH
Army Research Laboratory—WMRD AMSRL-WM-MD Aberdeen, Proving Ground, MD 21005-5069, USA

Devolatilization of the polymerization by-products and the impregnation solvent during Vacuum Assisted Resin Transfer Molding (VARTM) of the polyimide polymers is analyzed using a combined continuum hydrodynamics/chemical reaction one-dimensional model. The model which consists of seven coupled partial differential equations is solved using a finite element collocation method based on the method of lines. The results obtained reveal that the main process parameters which give rise to lower gas-phase contents in the VARTM-processed polymer matrix composites are the vacuum pressure and the tool-plate heating rate. Lower tool-plate heating rates are found to be beneficial since hey promote devolatilization of the impregnation solvent at lower temperatures at which the degree of polymerization and, hence, resin viscosity are low.

1. Introduction

Manual lay-up of pre-impregnated fibers over a mold surface followed by introduction of the resin using a brush or roller is quite common in manufacturing of advanced composite structures. However this process tends to be very expensive, and suffers from limited pre-preg shelf lives and short lay-up times. In addition, the process is highly labor intensive and quality control is difficult since the quality of the final product is highly dependent on the operator skills. Many of these limitations are eliminated in the Vacuum Assisted Resin Transfer Molding (VARTM) process which generally reduces lay-up times and makes the fabrication process more reproducible and consistent and less dependent upon operator skills.

VARTM is an advanced fabrication process for polymer-matrix composite structures which is used in (ground-based and marine) commercial and military applications [1–3]. The process has been developed over the last decade and has clear advantages over the traditional Resin Transfer Molding (RTM) process since it eliminates the costs associated with matched-metal tooling, reduces volatiles emission and allows the use of lower resin injection pressures [4]. The VARTM process whose schematic is shown in Fig. 1, typically involves the following three steps: (a) lay-up of a fiber preform (woven carbon or glass fabric) onto a rigid tool plate surface. The tool plate is surrounded by a formable vacuum bag; (b) impregnation of the preform with resin. The resin is injected through either a single or multiple inlet ports (depending on the part size and shape) and transferred into the preform by a pressure gradient (induced by the vacuum pressure), and by gravity and capillary effects; and (c) curing of the impregnated preform.

Porosity within polymer matrix composites (including the ones fabricated by the VARTM process) has long been recognized as a major limitation to the widespread use of these materials in many structural applications. Growth and coalescence of the pores under load can give rise to the formation of cracks and, in turn, result in premature failure. For epoxy matrix composites, it is generally recognized that environmentally-absorbed water is the primary cause for the formation of voids during processing. In the polymeric materials based on condensation polyimide systems, on the other hand, water and ethyl alcohol are formed as by-products of the polymerization reaction. In addition, significant amounts of an impregnation solvent, such as N-methyl-2-pyrolidone (NMP), are used in the polyimide systems during processing. Thus, to prevent void formation in these systems, the volatile polymerization by-products and the impregnation solvent must be removed from the reacting polymer before the part fabrication is completed. To produce void-free highperformance composites, the devolatilization process must be fully understood and controllable by (on-line) adjustment of the process parameters.

*Author to whom all correspondence should be addressed.

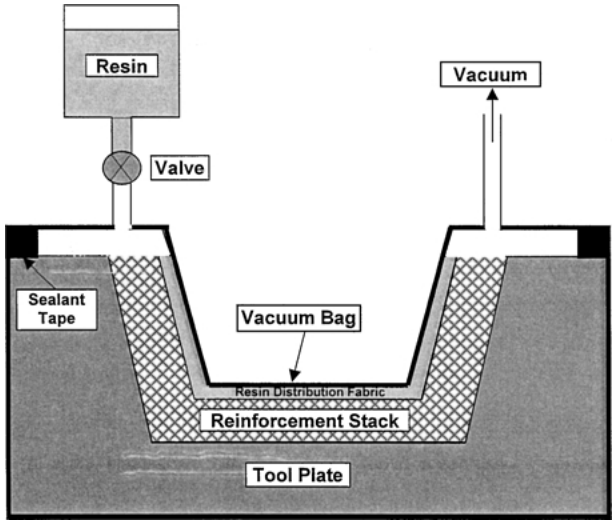

Figure 1 A schematic of the vacuum assisted resin transfer molding (VARTM) process.

To analyze the polymerization of polyimide systems during the VARTM fabrication process and help identify the optimum process parameters which ensure minimal porosity in the final product, a mathematical model for this process has been developed and utilized in the present work. It should be noted that the polymerization process in the polymide systems considered in the present work is quite complex since: (a) it takes place in a non-ideal solution of the impregnation solvent, monomers, polymeric fragments and the polymerization by-products; (b) the solvent and the polymerization by-products vaporize from the liquid phase; (c) solid polymer precipitate (and perhaps crystallize) within the liquid phase giving rise to a continuous change in the rheological and transport properties of the liquid phase; (d) heat, mass and momentum transport all occur in a three-phase reacting system within a consolidating fiber network; etc. In order to make modeling of the VARTM process mathematically tractable, a number of simplifying assumptions had to be introduced. The potential consequences of such assumptions are discussed in the paper.

The organization of the paper is as follows. In Sections 2.1 and 2.2, brief descriptions are given of the polyimide system (DuPont's Avimid K-III linear polymide) and the associated fiber-reinforced composite material studied in the present work. The model for the VARTM process consisting of seven coupled partial differential equations governing the behavior of the system under investigation is presented in Section 2.3. A brief overview of the finite element collocation method based on the method of lines is given in Section 3.4 The main results obtained in the present work are presented and discussed in Section 3, while the key conclusion resulting from the present work are summarized in Section 4.

2. Computational procedure

2.1. The basics of imide polymerization

Avimid K-III polymers are linear polyimides produced by condensation polymerization from an aromatic diethylester diacid (diethyl pyromellitate) and an aromatic ether diamine (4,4(1,1-biphenyl)-2,5-diyl-bis(oxy)bis(benzeneamine)) in a solvent typically consisting of phthalic anhydride (1 wt%), ethanol (1 wt%) and NMP (98 wt%). A schematic of the polymerization (imidization) reaction is given in Fig. 2 where it is seen that water and ethanol polymerization by-products and the impregnation solvent (NMP) vaporize and form the gas phase.

The kinetics of the imidization reaction is very complex due to the fact that the physical state of the material (e.g., polymer-chain flexibility) changes continuously during the polymerization as a result of solvent loss and cyclization (imidization) of the monomers. While the exact kinetics of the Avimid K-III is not known, Differential Scanning Calorimetry (DSC) measurements have shown that the imide formation reaction begins at $\sim$390 K and that it is completed at $\sim$ 450 K [5]. One of the most characteristic features of the imidization reaction is that its rate undergoes a sharp drop at a certain (temperature dependent) degree of imidization.

2.2. A representative material element for the Avimid K-III thermoplastic matrix fiber-reinforced composite

A two-dimensional representative material element (RME) of the fiber-reinforced Avimid K-III composite material fabricated by the VARTM process is shown schematically in Fig. 3. The height of the RME is equal to the thickness of the part while its width is generally much smaller and scales with the periodicity of the fiber-preform architecture in the horizontal direction. The RME contains three phases denoted as the solid fiber preform (S), the liquid resin (L) and the gas (G). The solid phase is considered as inert and rigid and to be surrounded by the liquid and gas phases. The gas phase

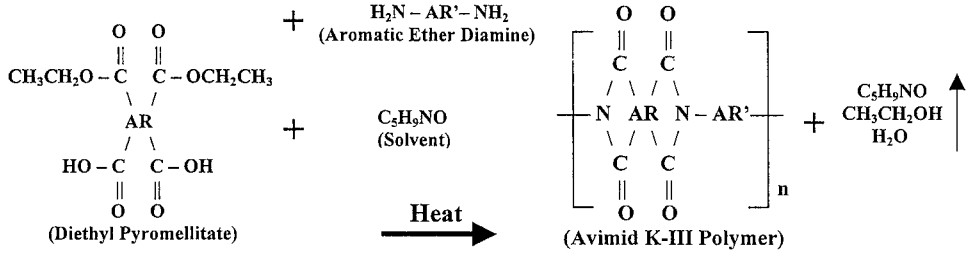

Figure 2 Polymerization chemistry of the Avimid K-III.

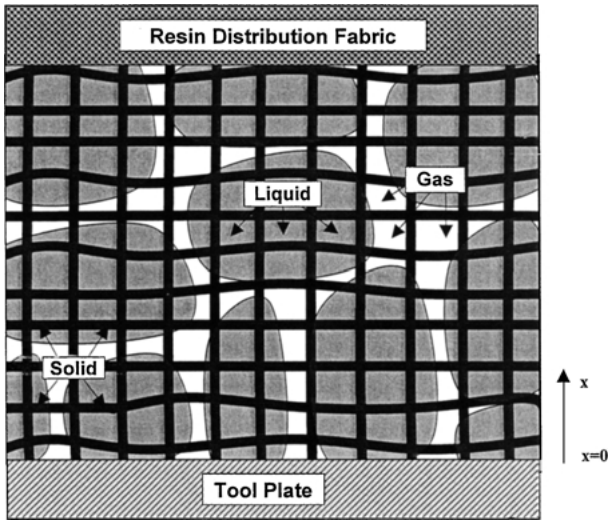

Figure 3 A representative material element (RME) for the Avimid K-III produced by the VARTM process.

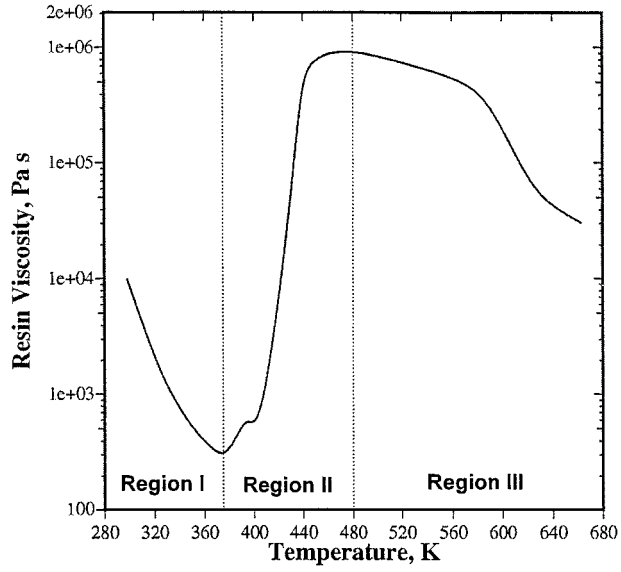

Figure 4 The effect of temperature on viscosity of the Avimid K-III resin [6].

is shown in Fig. 3 as a continuous phase. This is strictly valid only during the initial stages of the devolatilization process. Near the completion of part fabrication when most of the gas has been removed, the gas phase becomes discontinuous and consists of discrete bubbles. Hence, the model developed in the present work would have to be modified before it could be applied to the later stages of the VARTM process.

2.3. A model for imide polymerization during the VARTM process

2.3.1. Basic assumptions

The model developed in the present work is based on the following simplifying assumptions: (a) the solid phase is inert and its location within a RME is fixed; (b) the change in the laminate thickness during the VARTM process is small and can be neglected; (c) polymerization occurs by step reaction and only in the liquid phase; (d) transport by diffusion in the liquid and the gas phases and by convection in the liquid phase can be neglected relative to the convective transfer in the involved gas phase. The variation of the Avimid K-III resin viscosity with temperature displayed in Fig. 4 [6] shows that there are three distinct temperature regions: At temperatures below ∼390 K, Region 1, viscosity of the un-polymerized resin decreases with an increase in temperature. At temperatures between ∼390 K and ∼510 K, Region 2, the polymerization process takes place and, consequently, viscosity increases with an increase in temperature. At temperatures in excess of ∼510 K, Region 3, the polymerized resin begins to melt and, hence, its viscosity decreases with an increase in temperature. The data shown in Fig. 4 suggest that diffusion may become important toward the end of the VARTM process (Region 3) when the gas phase is not continuous any longer but rather consists of discrete bubbles. However, the role of diffusion in the overall management of the volatiles during the VARTM process in not expected to be significant; and (e) the gas phase can be considered as thermodynamically ideal.

Since the part (laminate) thickness is generally considerably smaller than its lateral dimensions, the VARTM process is analyzed using a one-dimensional model in which the principal (x) direction is chosen to be perpendicular to the tool plate. The perform is assumed to be instantaneously infiltrated with the resin and, at time equal to zero, the perform, the resin, distribution fabric and the tool plate are all assumed to be at the same temperature, $T_o = 353$ K. Then the temperature of the tool plate is increased at a constant rate, while a constant vacuum is applied at the resin distribution side of the laminate. The subsequent evolution of the material state and of other field quantities (temperature, pressure, gas-phase velocity, etc.) throughout the laminate thickness can be described using the appropriate heat, mass and momentum conservation equations within each of the three phases. However these equations cannot be generally solved due to the complex (discontinuous) microstructure (morphology) of the three-phase composite material. To overcome this problem, the composite morphology is homogenized using the method of volume averaging [6]. This enables the point-type equations (applicable to the composite materials with a discontinuous morphology) to be replaced by the corresponding volume-averaged continuity equations (applicable for the volume-averaged continuum representation of the composite material).

2.3.2. Governing equations

2.3.2.1. Energy conservation equation. Under the assumption of a local thermal equilibrium at each material point, the heat transfer between the resin and the fiber preform can be neglected and the temperature evolution is described by the following energy continuity equation:

$$\rho_m C_{pm} \frac{\partial T}{\partial t} + \rho_G C_{pG} V_G \frac{\partial T}{\partial x} + \sum_{i=1}^{3} (-\Delta H_{vap,i}) \dot{m}_i = k_m \frac{\partial^2 T}{\partial x^2} \quad (i = \text{NMP, ethanol, water}) \quad (1)$$

where T is the temperature, t the time, x the spatial coordinate perpendicular to the tool plate, ρ the mass density, C_p is the constant-pressure mass heat capacity, V the gas-phase velocity, ΔH_{vap} the mass heat of vaporization, $\dot{m}$ the volatilization mass flux and k the thermal conductivity. Subscripts m, G and i are used to denote volume averages of the 3-phase (fiber, resin, gas) mixture (composite), the gas phase and the volatile components (NMP, ethanol, water), respectively.

The first term on the left-hand side of the Equation 1 represents the rate of change of the internal energy per unit volume, the second term accounts for the convective gas-phase heat transfer, the third term represents the energy sink associated with the evaporation of the volatile species. The conductive heat transfer is represented by the right-hand side of Equation 1.

The volume-averaged constant-pressure (volumetric) heat capacity and thermal conductivity of the composite material are respectively defined as:

$$\rho_m C_{pm} = \varepsilon_S \rho_S C_{pS} + \varepsilon_L \rho_L C_{pL} + \varepsilon_G \rho_G C_{pG} \quad (2)$$

and

$$k_m = \varepsilon_S k_S + \varepsilon_L k_L + \varepsilon_G k_G \quad (3)$$

where ε_S, ε_L, and ε_G denote volume fractions of the solid, liquid and gas phases in the composite material, respectively. Analogous relations are used to compute the volume-averaged effective constant-pressure heat capacity and thermal conductivity of the liquid and the gas phases as functions of the volume fractions of their constituents. The constituents of the liquid phase are diamine, diacid, polymer, NMP, ethanol and water while the constituents of the gas phase are NMP, ethanol and water.

Equation 1 is subjected to the following initial and boundary conditions:

$$\text{I.C.} \qquad T(x, t=0) = T_o \quad (4)$$

$$\text{B.C. (1)} \quad T(x=0, t) = T_o + \int_0^t \alpha \, dt \quad (5)$$

$$\text{B.C. (2)} \quad -k_m \frac{\partial t}{\partial t}\bigg|_{x=L} = h(T(x=L, t) - T_{df}) \quad (6)$$

where $x = 0$ corresponds to the tool-plate/composite interface, L is the laminate thickness, T_o the initial temperature, α the heating rate of the tool plate, h the composite/resin-distributive-fabric heat transfer coefficient and T_{df} the temperature of the resin distribution fabric.

The initial condition given by Equation 4 states that the composite is initially at uniform temperature. The first boundary condition, Equation 5, is based on the assumption of a negligible contact thermal resistance between the tool plate and the composite and equates the composite temperature at the tool-plate/composite interface to that of the tool plate. The second boundary condition, Equation 6, postulates that heat transfer from the composite to the distribution fabric is controlled by convection.

2.3.2.2. Overall liquid-phase mass conservation equation. Under the assumption that diffusion and convection in the liquid phase can be neglected, the liquid-phase mass conservation is defined as a balance of the accumulation and the reaction (evaporation) terms as:

$$\rho_L \frac{\partial \varepsilon_L}{\partial t} + \varepsilon_L \frac{\partial \rho_L}{\partial t} = -\sum_{i=1}^{3} \dot{m}_i \quad (i = \text{NMP, ethanol, water}) \quad (7)$$

where ρ_L is the overall density of the liquid phase which is a function of the composition of the liquid phase as:

$$\rho_L = \sum_{i=1}^{6} \phi_i \rho_{Li} \quad (i = \text{NMP, ethanol, water, diamine, diacid, polymer}) \quad (8)$$

and ϕ_i and ρ_{Li} are respectively the volume fraction and the density of the liquid-phase species i. The second term on the left-hand side of Equation 7 is generally small and can be neglected. Also, since the gas phase is initially not present, the following initial condition can be defined:

$$\text{I.C.} \quad \varepsilon_L(x, t=0) = 1 - \varepsilon_S^o \quad (9)$$

where ε_S^o is the fixed volume fraction of the solid phase (fiber preform).

2.3.2.3. Mass balance of water and ethanol in the liquid phase. As discussed earlier, water and ethanol are formed as by-products of the imidization reaction and also evaporate during the VARTM process. Therefore their mass balances involve the accumulation, reaction and devolatilization terms as:

$$\varepsilon_L \frac{\partial C_{H_2O}}{\partial t} = 2R_A \varepsilon_L - C_{H_2O} \frac{\partial \varepsilon_L}{\partial t} - \frac{\dot{m}_{H_2O}}{MW_{H_2O}} \quad (10)$$

and

$$\varepsilon_L \frac{\partial C_{CH_3CH_2OH}}{\partial t} = 2R_A \varepsilon_L - C_{CH_3CH_2OH} \frac{\partial \varepsilon_L}{\partial t} - \frac{\dot{m}_{CH_3CH_2OH}}{MW_{CH_3CH_2OH}} \quad (11)$$

where C_{H_2O} and $C_{CH_3CH_2OH}$ are the molar concentrations of water and ethanol, respectively, R_A the rate of destruction of the active (monomer) groups, and MW is used to denote the molecular weight. The factor 2 in front of R_A in Equations 10 and 11 is used to indicate that two moles of water and two moles of ethanol are formed for each mole of the active groups consumed. Since the resin may contain environmentally adsorbed water and ethanol is often deliberately used as a component of the impregnation solvent, Equations 10 and 11 are respectively subject to the following initial conditions:

$$\text{I.C. (1)} \quad C_{H_2O}(x, t=0) = C_{H_2O}^O \quad (12)$$

$$\text{I.C. (2)} \quad C_{CH_3CH_2OH}(x, t=0) = C_{CH_3CH_2OH}^O \quad (13)$$

2.3.2.4. Mass balance of NMP in the liquid phase. NMP is the main component of the impregnation solvent and evaporates during the VARTM process, but it is not a by-product of the imidization reaction. Hence, its balance involves the accumulation and devolatilization terms as:

$$\varepsilon_{\mathrm{L}}\frac{\partial C_{\mathrm{NMP}}}{\partial t} = -C_{\mathrm{NMP}}\frac{\partial \varepsilon_{\mathrm{L}}}{\partial t} - \frac{\dot{m}_{\mathrm{NMP}}}{MW_{\mathrm{NMP}}} \tag{14}$$

and, hence, the corresponding initial condition can be defined:

$$\text{I.C.} \quad C_{\mathrm{NMP}}(x, t=0) = C^{\mathrm{O}}_{\mathrm{NMP}} \tag{15}$$

where $C^{\mathrm{O}}_{\mathrm{NMP}}$ is the initial concentration of NMP in the liquid phase.

2.3.2.5. Mass balance of the active groups. If the total (molar) concentration of active groups present in the monomer and growing polymer chains, is denoted as C_{A}, the mass balance of the active groups and the corresponding initial condition can be defined as:

$$\varepsilon_{\mathrm{L}}\frac{\partial C_{\mathrm{A}}}{\partial t} = -R_{\mathrm{A}}\varepsilon_{\mathrm{L}} - C_{\mathrm{A}}\frac{\partial \varepsilon_{\mathrm{L}}}{\partial t} \tag{16}$$

and

$$\text{I.C.} \quad C_{\mathrm{A}}(x, t=0) = C^{\mathrm{O}}_{\mathrm{A}} \tag{17}$$

where, $C^{\mathrm{O}}_{\mathrm{A}}$ is the initial concentration of the diamine (diacid).

2.3.2.6. Overall mass balance of the gas phase. Under the assumption that diffusion in the gas phase is negligible in comparison to the pressure-gradient driven convection, the overall gas-phase mass conservation can be described as:

$$\frac{\partial}{\partial t}(\rho_{\mathrm{G}}\varepsilon_{\mathrm{G}}) + \frac{\partial}{\partial x}(\rho_{\mathrm{G}}V_{\mathrm{G}}) = \sum_{i=1}^{3}\dot{m}_{\mathrm{i}} \quad (i = \text{NMP, ethanol, water}) \tag{18}$$

Using the Darcy's law to describe the relationship between the gas-phase velocity, V_{G}, and the pressure gradient, $\frac{\partial P}{\partial x}$:

$$V_{\mathrm{G}} = \frac{k_{\mathrm{G}}}{\mu_{\mathrm{G}}}\frac{\partial P}{\partial x}, \tag{19}$$

the ideal-gas law to define the density of the gas phase:

$$\rho_{\mathrm{G}} = \frac{PMW_{\mathrm{G}}}{RT}, \tag{20}$$

and the relation:

$$\varepsilon_{\mathrm{s}} + \varepsilon_{\mathrm{L}} + \varepsilon_{\mathrm{G}} = 1 \tag{21}$$

Equation 18 can be rewritten as:

$$\frac{\varepsilon_{\mathrm{G}}}{RT}\frac{\partial P}{\partial t} = \frac{1}{MW_{\mathrm{G}}}\sum_{i=1}^{3}\dot{m}_{\mathrm{i}} + \frac{P}{RT}\left(\frac{\partial \varepsilon_{\mathrm{L}}}{\partial t} + \frac{k_{\mathrm{G}}}{\mu_{\mathrm{G}}}\frac{\partial^2 P}{\partial x^2}\right) + \frac{\varepsilon_{\mathrm{G}}P}{RT^2}\frac{\partial T}{\partial t} + \frac{k_{\mathrm{G}}}{\mu_{\mathrm{G}}}\frac{\partial P}{\partial x}\left(\frac{1}{RT}\frac{\partial P}{\partial x} - \frac{P}{RT^2}\frac{\partial T}{\partial x}\right) \tag{22}$$

where R is the universal gas constant, while k_{G} is permeability of the resin-infiltrated perform, μ_{G} is the gas-phase viscosity and MW_{G} is the mean gas-phase molecular weight.

The initial and the boundary conditions for Equation 22 can be defined as:

$$\text{I.C.} \quad P(x, t=0) = P_{\mathrm{o}} \tag{23}$$

$$\text{B.C. (1)} \quad \frac{\partial P}{\partial x}(x=0, t) = 0 \tag{24}$$

$$\text{B.C. (2)} \quad P(x=L, t) = P_{\mathrm{vac}} \tag{25}$$

where P_{o} and P_{vac} are the initial pressure and the applied vacuum pressure at the resin distribution-fabric side of the composite respectively.

2.3.3. System-dependent constitutive relations

Equations 1, 7, 10, 11, 14, 16 and 22 represent a system of seven coupled partial differential equations with seven unknowns: T, ε_{L}, $C_{\mathrm{H_2O}}$, $C_{\mathrm{CH_3CH_2OH}}$, C_{NMP}, C_{A} and P. Before these equations can be solved, additional, material-system dependent constitutive equations are required to define the evaporation rates of the volatile species ($\dot{m}$), the rate of destruction of the active groups (R_{A}), and the dependencies of permeability (k_{G}) and viscosity (μ_{G}) on the degree of polymerization. These equations are defined below:

2.3.3.1. Evaporation rates of the volatile species. Following Yang *et al.* [6], the evaporation rate of the i-th volatile component can be defined as:

$$\dot{m}_{\mathrm{i}} = (K_{\mathrm{m}}A_{\mathrm{L}})_{\mathrm{i}}\left(\gamma_{\mathrm{i}}\phi_{\mathrm{i}}P^{\mathrm{sat}}_{\mathrm{i}} - Y_{\mathrm{i}}P\right) \tag{26}$$

where K_{m} is the liquid/gas mass transfer coefficient, A_{L} the liquid/gas interfacial area per unit volume of the composite material, γ_{i}, ϕ_{i} and $P^{\mathrm{sat}}_{\mathrm{i}}$ the activity coefficient, the volume fraction and the saturation pressure of species i in the liquid phase and Y_{i} the molar fraction of the species i in the gas phase. Procedures used to calculate the parameters appearing on the right hand side of Equation 26 are discussed below.

The overall liquid/gas mass transfer coefficient, $K_{\mathrm{m}}A_{\mathrm{L}}$, is one of the key parameters controlling the rate of devolatilization. As devolatilization proceeds, the gas/liquid interfacial area increases, while the mass transfer coefficient K_{m} decreases due to a polymerization-induced increase of the resin viscosity. Consequently, the volumetric mass transfer coefficient,

$K_m A_L$, experiences a maximum at a temperature T_{max}. The temperature dependence of $K_m A_L$ in kg/m^3/s/Pa was experimentally determined by Yoon *et al*. [5] as:

$$K_m A_L = 7.5 \times 10^{-7} \sin\left[\frac{\pi}{2}\left(\frac{T}{T_{max}}\right)^2\right] \quad \text{for } T \le T_{max} \tag{27}$$

$$K_m A_L = 7.5 \times 10^{-7} \sin\left[\frac{\pi}{2}\left(\frac{T}{T_{max}}\right)^4\right] \quad \text{for } T \ge T_{max} \tag{28}$$

Yoon *et al*. [5] also reported that T_{max} increases moderately with the (constant) heating rate (T_{max} (α = 0.6 K/min) = 403 K and (T_{max} (α = 2.2 K/min) = 423 K).

The activity coefficient γ_i can be calculated using the Flory-Huggins equation [8] as:

$$\gamma_i = \exp\left[\left(1 - \frac{1}{\bar{x}_n}\right)\phi_p + \chi\phi_p^2\right] \tag{29}$$

where ϕ_P is the combined volume fraction of the monomer and the polymer, $\bar{x}_n$ the mean number of mers in the polymer chains (including monomers) and χ a molecular interaction parameter whose value typically falls into a range between 0.2 and 0.5. Following Yoon *et al*. [5], $\chi = 0.35$ is used for the Avimid K-III system under consideration. The mean number of mers in the polymer chains is related to the degree of polymerization p ($= (C_A^o - C_A)/C_A^o$) as:

$$\bar{x}_n = \frac{1}{1-p} \tag{30}$$

Equation 28 is based on an assumption that the molecular size distribution in a polymer can be represented by a geometric probability function which is generally accepted as a reasonably good approximation for condensation polymers such as Avimid K-III.

The vapor pressures P_i^{sat} of the pure volatile components of the liquid (NMP, methanol and water) at different temperatures have been computed using the Clausius-Clapeyron equation [9] and the available heat of evaporation and boiling point data for these components as:

$$P_i^{sat} = \exp\left(-\frac{\Delta H_{vap,i}/T - \Delta H_{vap,i,o}/T_{b,i}}{R}\right) \quad (i = \text{NMP, ethanol, water}) \tag{31}$$

where $\Delta H_{vap,o}$ is the heat of evaporation at the boiling point T_b. The temperature dependence of the heat of evaporation has been obtained using the Watson's correlation [9] as:

$$\Delta H_{vap,i} = \Delta H_{vap,i,o} * \left(\frac{1 - T/T_{C,i}}{1 - T_b/T_{C,i}}\right)^n \quad (i = \text{NMP, ethanol, water}) \tag{32}$$

where T_C is the critical temperature and the exponent n is assigned its standard value of 0.38 [9].

Since it is generally found that evaporation flux dominates the mass balance of the volatile species during devolatilization, the molar fraction Y_i of each volatile component i in the gas phase can be approximated as:

$$Y_i = \frac{\dot{m}_i/MW_i}{\sum_{i=1}^{3} \dot{m}_i/MW_i} \quad (i = \text{NMP, ethanol, water}) \tag{33}$$

2.3.3.2. Rate of destruction of the active groups. As stated earlier, the exact kinetics for polymerization of the Avimid K-III polyimide system is not well established. Following Yoon *et al*. [5], the rate of destruction of the active groups, R_A, is approximated using a first-order kinetic equation as:

$$R_A = -\frac{dC_A}{dt} = k_A C_A \tag{34}$$

in which the reaction-rate constant k_A is defined as:

$$\ln(k_A) = A_0 + A_i \ln(t) + \frac{A_2}{T} \tag{35}$$

For k_A in min^{-1}, T in K and t in min, the three constants in Equation 35 take on the following values: $A_0 = 31.2113$, $A_1 = -0.1888$ and $A_2 = -13.6 \times 10^3$ for the Avimid K-III system [5].

2.3.3.3. Changes in condensed-phase permeability and gas-phase viscosity. As the polymerization proceeds, condensed-phase permeability k_G decreases and in the absence of a more accurate model has been assumed to be a linear function of the degree of polymerization, p. The viscosity, μ_G, on the other hand, is fully reflected by the properties of the gas phase and is assumed to be given as a volume-average temperature-dependent viscosities of the gas-phase components.

2.4. Finite element collocation method

The system of seven coupled partial differential equations which govern the behavior of the Avimid K-III system during the VARTM fabrication process is solved using a finite element collocation method based on the method of lines [10]. Within this method, the spatial domain (the x-direction) is discretized into elements and the x-dependent portion of the solution represented using a polynomial basis function. The polynomial coefficients are, on the other hand, time dependent. By requiring that the solutions to the system of partial differential equations (PDE's) satisfy the boundary conditions and the continuity conditions at the nodal points separating the elements, the system of PDE's is converted into a semi-discrete system of Ordinary Differential Equations (ODEs) which depend only on time. These equations are then integrated using a standard integration procedure to determine the unknown time-dependent polynomial coefficients at a new time step in terms of the solution at the previous time step.

TABLE I Properties of the components of the liquid phase

Property	Symbol	Unit	Diamine	Diacid	NMP	Ethanol	Water
Density	ρ	kg/m^3	0.994×10^3	1.24×10^3	1.03×10^3	0.79×10^3	1.0×10^3
Heat capacity	C_p	J/kg/K	0.345×10^3	1.68×10^3	1.67×10^3	2.43×10^3	4.18×10^3
Thermal conductivity	k	W/m/K	0.25	0.25	1.79	0.19	0.603
Molecular weight	MW	kg/mol	368.43×10^{-3}	310.0×10^{-3}	99.1×10^{-3}	46.1×10^{-3}	18.0×10^{-3}
Molar volume	V^m	m^3/mol	370.65×10^{-6}	250×10^{-6}	96.49×10^{-6}	58.39×10^{-6}	18.02×10^{-6}
Boiling point	T_b	K	N/A[a]	N/A[a]	477.3	351.4	373.0
Heat of vaporization at T_b	$\Delta H_{vap,o}$	J/kg	N/A[a]	N/A[a]	510.5×10^3	854.0×10^3	2256.0×10^3
Critical temperature	T_c	K	N/A[a]	N/A[a]	721.7	516.3	647.4

[a]Data not needed since evaporation of Diamine and Diacid is not considered.

TABLE II Properties of the components of the gas phase

Property	Symbol	Unit	NMP	Ethanol	Water
Heat capacity	C_p	J/kg/K	1.26×10^3	1.43×10^3	2.02×10^3
Thermal conductivity	k	W/m/K	1.79	0.19	0.603
Molecular weight	MW	kg/mol	99.1×10^{-3}	46.1×10^{-3}	18.0×10^{-3}
Viscosity	μ_G	Ns/m^2	1.67×10^{-3}	1.10×10^{-3}	0.89×10^{-3}

TABLE III Typical VARTM processing parameters for Avimid K-III material composite

Parameter	Symbol	Units	Value	Equation where first used
Volume fraction of solid	ε_S	N/A	0.58	2
Initial temperature	T_o	K	333.0	4
Tool-plate heating rate	α	K/min	0.5–2.0	5
Laminate thickness	L	m	0.0064	6
Tool-plate/composite heat transfer coefficient	h	W/m^2/K	27.9	6
Initial concentration of water	$C^o_{H_2O}$	mol/m^3	0.0	12
Initial concentration of ethanol	$C^o_{CH_3CH_2OH}$	mol/m^3	2.59×10^2	13
Initial concentration of NMP	C^o_{NMP}	mol/m^3	2.41×10^3	15
Initial concentration of active groups	C^o_A	mol/m^3	1.39×10^3	17
Condensed phase permeability for the gas phase	k_G	m^2	3.0×10^{-15}–$2.85 \times 10^{-15} p$	22
Applied vacuum	P_{vac}	Pa	6666.7	25

3. Results and discussion

All the calculations carried out in the present work pertain to an Avimid K-III matrix composite material reinforced with 58 vol% of carbon fiber performs. Consequently, the following (typical) properties are assigned to the solid phase [11]: $\rho_S = 1940$ kg/m^3, $C_{pS} = 750$ J/kg/K and $k_S = 10$ W/m/K. Properties of the liquid and the gas components are given in Tables I and II, respectively. Typical values and ranges of the VARTM processing parameters used in the present work are summarized in Table III.

3.1. Analysis of devolatilization under typical VARTM processing conditions

The model described in Section 2.3 is used in this section to analyze devolatilization of the water, ethanol and NMP during VARTM processing of Avimid K-III matrix carbon fiber reinforced composites under typical processing conditions. In the following, the results obtained are presented and briefly discussed.

Variations of temperature, pressure, the degree of polymerization and the volume fraction of the gas phase throughout the laminate thickness at different times following infiltration (assumed to occur at a time $t = 0$) of the carbon fiber perform with resin are shown in Fig. 5a–d, respectively. All the results shown in Fig. 5a–d are obtained under a constant (1 K/min) heating rate of the tool-plate.

The results displayed in Fig. 5a show that at any instant during VARTM processing of the Avimid K-III matrix carbon fiber reinforced composites, the temperature variation throughout the laminate thickness is quite small, typically not exceeding 4 K. This finding is reasonable considering the relatively small laminate thickness (0.0064 m) and the relatively small heating rate. The Biot number, which is defined as a ratio of the resistance to heat conduction through the laminate and the resistance to heat convection from the laminate to the resin-rich resin-distribution fabric is found to be around 0.03. Such a small value of the Biot number justifies the observed high uniformity in the temperature throughout the laminate thickness.

Variations of the gas-phase pressure throughout the laminate thickness at different times following perform infiltration with the resin is displayed in Fig. 5b. As expected, the pressure is the highest at the tool-plate/laminate interface and is constant and equal to the applied vacuum pressure (6666.7 Pa) at the resin-distribution fabric end of the laminate. It is also seen that the pressure initially increases as water and ethanol (generated as the polymerization by-products) and NMP solvent evaporate. However, as devolatilization of the gas phase at the laminate/distribution-fabric

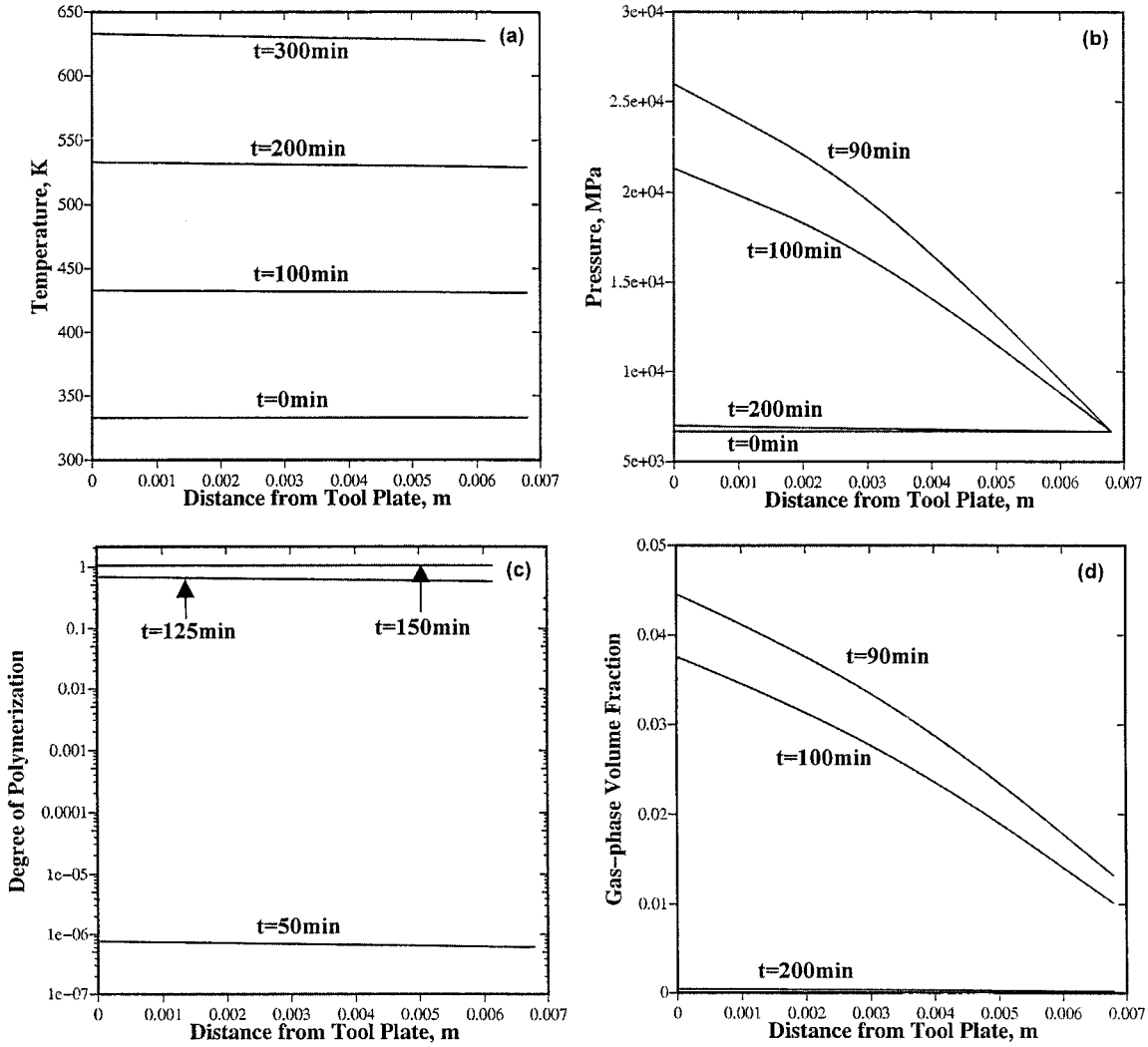

Figure 5 Variations of: (a) temperature, (b) pressure, (c) degree of polymerization, and (d) the volume fraction of the gas phase throughout the laminate thickness at different times following infiltration of the perform with resin. Heating rate = 1 K/min.

interface proceeds, the gas-phase pressure begins to decrease.

The results presented in Fig. 5c show that the distribution of the degree of polymerization throughout the laminate thickness is quite uniform which is consistent with the corresponding uniform temperature fields displayed in Fig. 5a.

A comparison of the results presented in Fig. 5b and d shows that the variation of the volume fraction of the gas phase throughout the laminate thickness at different times following perform infiltration with the resin closely matches the corresponding results for the gas-phase pressure.

The evolution of the pressure and degree of polymerization in the course VARTM processing of the Avimid K-III base carbon-fiber reinforced composites can be further understood by analyzing the results displayed in Fig. 6a and b. The results displayed in Fig. 6a show the variation of pressure at the tool-plate laminate interface as a function of tool-plate temperature under a constant (1 K/min) heating rate of the tool plate. As discussed earlier, evaporation of water, ethanol and NMP give rise to an increase in the gas-phase pressure at lower tool-plate temperatures. However, as devolatilization proceeds, the amount of volatiles in the liquid phase decreases and so does the gas-phase pressure. The results displayed in Fig. 6b show that the polymerization of the resin in contact with the tool-plate is complete by ~470 K. In addition a comparison of the results displayed in Fig. 6a and b shows that at the completion of polymerization, the gas phase pressure is still quite high (~10,000 MPa) and that, due to high viscosity of the fully-polymerized resin, the rate of pressure reduction by devolatilization has been substantially decreased.

Variations of the accumulated mass fluxes of water-vapor, ethanol, NMP and the (total) gas phase at the resin-distribution fabric end of the laminate as a function of temperature of the tool plate at three different heating rates are shown in Fig. 7a–d, respectively. The accumulated mass fluxes of the three gas-phase components at the resin-distribution fabric end of the composite material is given by the following equation:

$$Q_{\mathrm{i}} = V_{\mathrm{G}}\rho_{\mathrm{Gi}} \quad (i = \mathrm{NMP, ethanol, water}) \qquad (36)$$

where ρ_{Gi} is the density of i-th component of the gas phase. The total accumulated flux of the gas phase is defined as a sum of the accumulated mass fluxes of the three gas-phase components.

The results displayed in Fig. 7a–d show that the lower is the heating rate of the tool plate the larger is the accumulation flux of each of the three gas-phase components

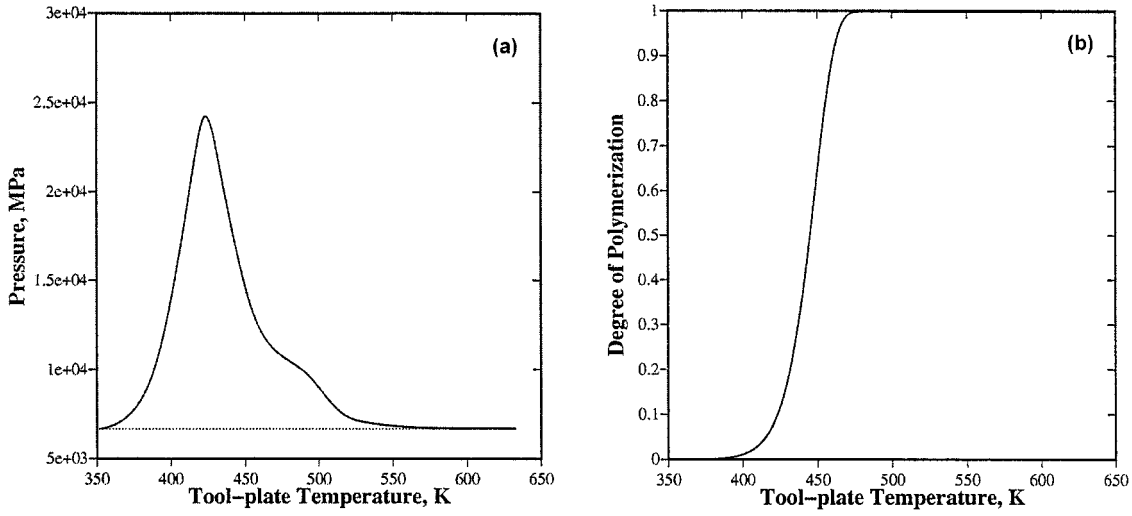

Figure 6 Variations of: (a) pressure and (b) degree of polymerization as a function of temperature at the tool-plate/laminate interface at a heating rate of 1 K/min.

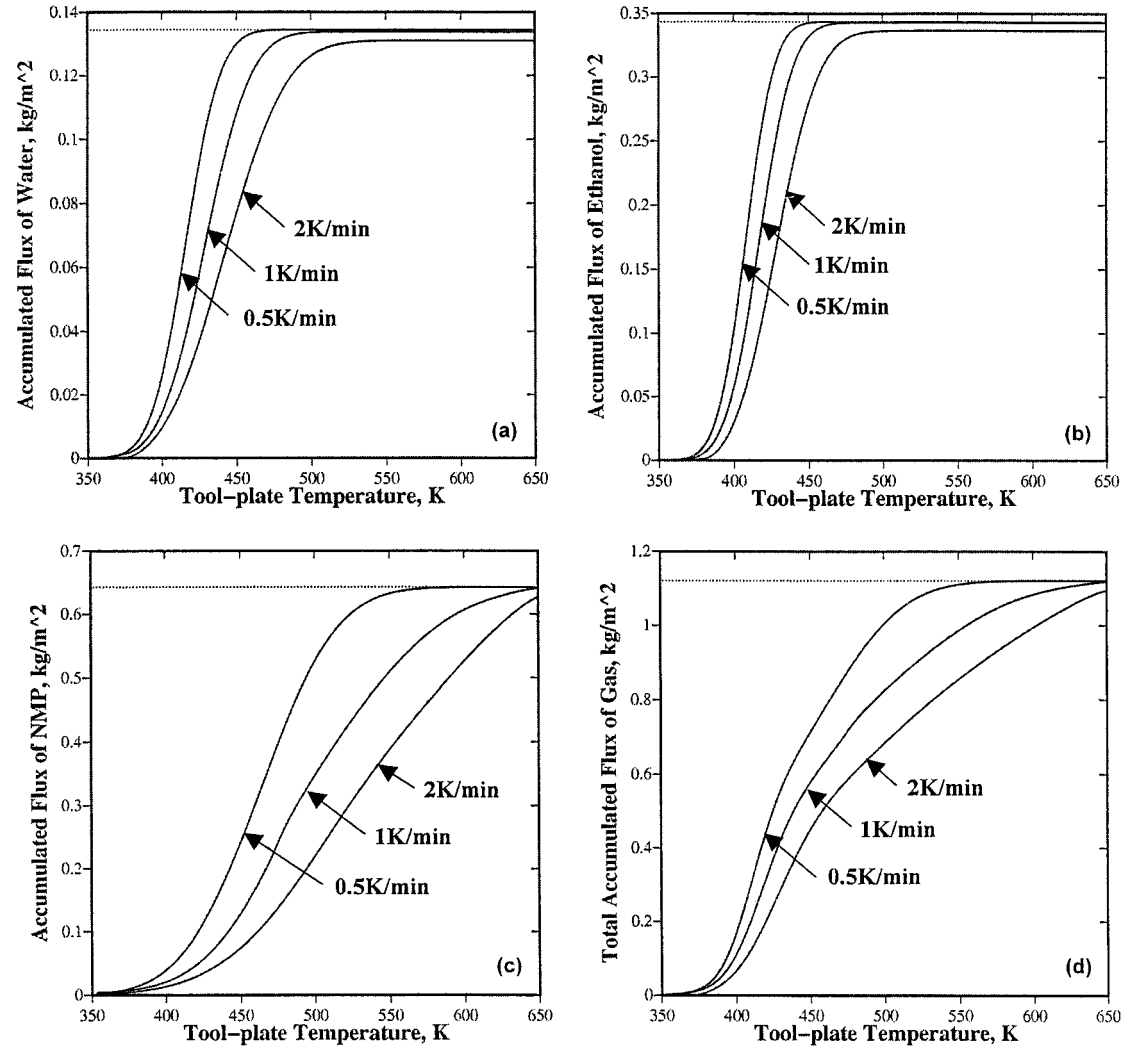

Figure 7 Variations of the accumulated fluxes for: (a) water vapor, (b) ethanol, (c) NMP, and (d) the gas phase as a function of temperature at the tool-plate/laminate interface at three different heating rates.

and, thus, the lower are the amounts of volatiles left in the composite at completion of the VARTM process. Hence, the use of lower heating rates is preferred from the standpoint of achieving a more complete removal of the gas-phase in VARTM-processed composites. On the other hand, the benefits of lower heating rates have to be balanced against the resulting longer part-manufacturing times and the associated higher manufacturing cost.

The effect of vacuum pressure P_{vac} is also studied in the present work but the results are not shown for brevity. The main finding of this portion of the

calculations is that, at a given tool-plate heating rate, the fraction of the gas phase left in the composite at the completion of the VARTM process decreases linearly with the vacuum pressure P_{vac}.

3.2. Optimization of the VARTM process

As discussed in the introduction, Section 1, the main objective of the present work is to develop a mathematical model of the VARTM process which can be used to optimize this process with respect to achieving the highest extent of devolatilization. From the findings and considerations presented in the previous section, it is clear that to achieve this goal, the extent of devolatilization of the volatile species (NMP in particular) should be maximized at lower temperature, while the degree of polymerization and, hence, the resin viscosity are low and the mass transfer coefficient (K_m) is high. As discussed earlier, to lower the resin viscosity and, thus, help ensure a complete perform infiltration with the resin, NMP solvent is mixed with diamine and diacid. Using the experimental measurements of the temperature dependence of viscosity of the Avimid K-III reported by Yoon [7], and the NMP viscosity value of 0.0016 kg/m/s, the following relation is obtained between the liquid-phase viscosity, μ_L, in kg/m/s, the temperature and the initial molar concentrations of the active groups and NMP in mol/m^3: Diamine

$$\mu_L = (431.91 - 6.9868T + 0.0318T^2) \times \frac{C_A^o\left(V_{Diamine}^m + V_{Diacod}^m\right)}{C_A^o\left(V_{Diamine}^m + V_{Diacod}^m\right) + C_{NMP}^\circ V_{NMP}^m} \quad (37)$$

where V^m is used to denote the molar volume in mol/m^3.

The functional relationship defined by Equation 37 is used to generate the liquid-phase viscosity contour plot shown in Fig. 8a for $C_A^o = 1.39 \times 10^3$ mol/m^3. As expected, liquid-phase viscosity is seen to decrease with an increase in temperature and an increase in the concentration of NMP. Using the experimental data for temperature dependences of the liquid-phase viscosity, the overall liquid/gas mass transfer coefficient, $K_m A_L$, and the volume fraction and the mean diameter of gas-phase bubbles in the resin, as reported by Yoon [7], the following relationship is derived between the mass transfer coefficient, K_m, in kg/m^5/Pa/s and the liquid-phase viscosity kg/m/s:

$$K_m = 0.1342 \times 10^{-10} - 0.1184 \times 10^{-13}\mu_L + 0.1187 \times 10^{-16}\mu_L^2 \quad (38)$$

The functional dependence between the mass transfer coefficient in kg/m^5/Pa/s, temperature and the NMP molar concentration is displayed using a contour plot in Fig. 8b. As expected, higher temperatures and higher NMP concentrations are seen to promote evaporation of the polymerization by-products and the NMP solvent by increasing the mass transfer coefficient.

Since, according to Equation 38, the mass transfer coefficient, K_m, increases with a decrease in the liquid-phase viscosity, an increased concentration of NMP in the liquid phase is preferred. However, an increase in the concentration of NMP in the liquid phase also means that a larger amount of the gas-phase will have to be removed from the composite through devolatilization. This implies that there is and optimum NMP concentration in the liquid phase which, at a given heating rate, gives rise to a maximum degree of gas-phase removal from the composite material.

The notion of the optimal concentration of NMP can be further understood by analyzing the contour plot shown in Fig. 9. In this figure, the fraction of volatiles left in the composites at the highest temperature attained during the VARTM process (taken to be 623 K for Avimid K-III matrix carbon fiber reinforced composites) is plotted as a function of the tool-plate heating rate and the molar concentration of NMP. It is seen that at each constant level of the fraction of volatiles left in the composite, there is and optimum concentration of NMP which is associated with the highest allowable tool-plate heating rate. A dashed line is used to connect the optimum NMP concentrations/heating rate points at different contour lines and, thus, to show that both the optimal NMP concentration and the corresponding highest heating rate decrease as the fraction of the

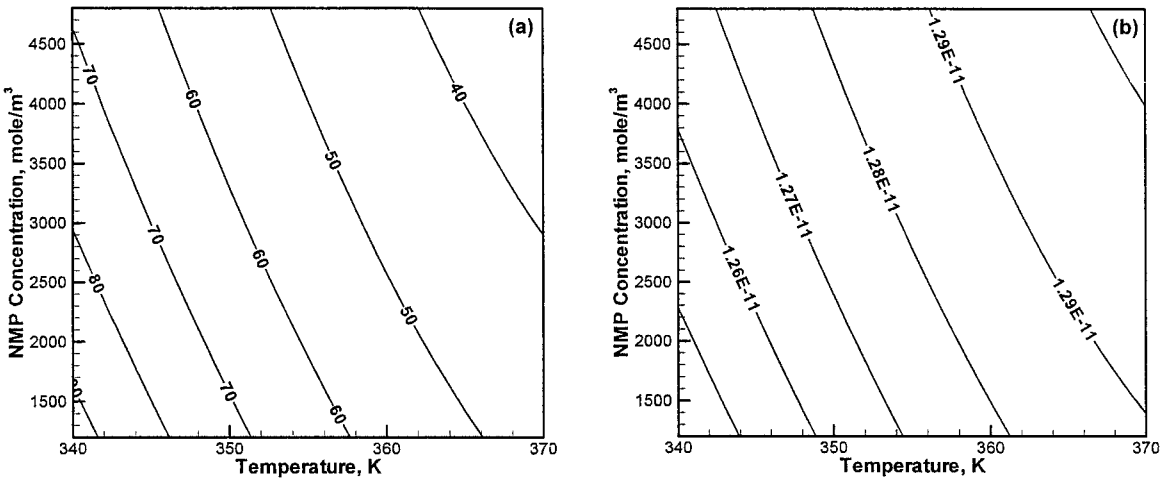

Figure 8 Variations of: (a) viscosity in kg/m/s of the liquid phase and (b) mass transfer coefficient in kg/m^5/Pa/s with temperature and molar concentration of NMP.

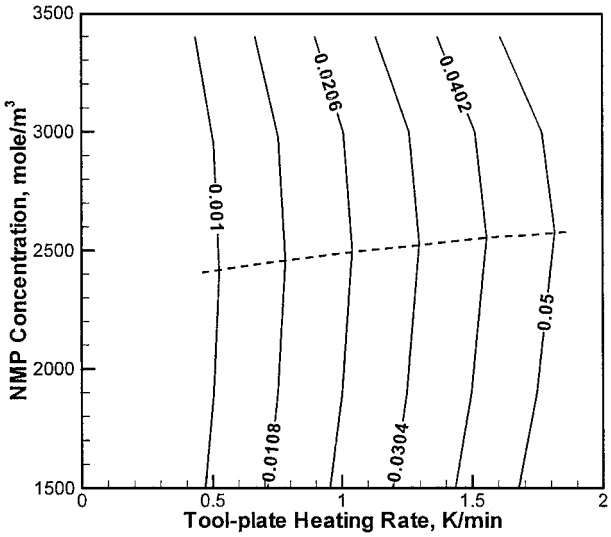

Figure 9 Contour plot of the volume fraction of gas phase left in the composite at the completion of the VARTM process as a function of the tool-plate heating rate and the initial molar fraction of NMP in the resin.

volatiles left in the composites decreases. However, the results displayed in Fig. 9 show that the increase in the tool-plate heating rate associated with the use of the optimum NMP concentration is quite small. Hence, the optimum concentration of NMP in the resin would be, in general, governed by the NMP's role in lowering resin viscosity and, thus, in promoting a complete perform infiltration with the resin rather than by the devolatilization aspects of the VARTM process.

4. Conclusions

Based on the results obtained in the present work, the following main conclusions can be drawn:

1. Adequate modeling of devolatilization during the VARTM process requires consideration of both chemical effects associated with polymerization of the resin and hydrodynamic effects associated with the transport of volatiles through the resin.

2. Lower tool-plate heating rates promote devolatilization of the volatiles (in particular, of the NMP solvent) at lower temperatures at which, due to a low degree of polymerization, resin viscosity is low. This results in a more complete removal of the volatiles and a lower gas-phase content in VARTM-processed fiber reinforced polymer matrix composites. However, lower too-plate heating rates are generally associated with higher manufacturing costs.

3. From the standpoint of achieving a high degree of gas-phase removal at a highest possible tool-plate heating rate, there is, in general, an optimum concentration of the solvent. However, the benefits of using the optimum NMP concentration relatively to increasing the tool-plate heating rate and, thus, in reducing the VARTM processing time, are relatively limited.

Acknowledgements

The material presented in this paper is based on work supported by the U.S. Army Grant Number DAAD19-01-1-0661. The authors are indebted to Drs. Walter Roy, Fred Stanton, William DeRosset and Dennis Helfritch of ARL for the support and a continuing interest in the present work. The authors also acknowledge the support of the Office of High Performance Computing Facilities at Clemson University.

References

1. S. M. LEWIT and J. C. JAKUBOWSKI, SAMPE International Symposium, (1997) Vol. 42, p. 1173.
2. L. B. NQUYEN, T. JUSKA and S. J. MAYES, AIAA/ASME/ASCE/AHS/ASC Structures, Structural Dynamics and Materials Conference (1997) Vol. 38, p. 992.
3. P. LAZARAS, SAMPE International Symposium (1996) Vol. 41, p. 1447.
4. J. R. SAYRE, "RFI and SCIMP Model Development and Verification," PhD thesis, Virginia Polytechnic Institute and State University, Blacksburg, VA, 2000.
5. I. S. YOON, Y. YANG, M. P. DUDUKOVIC and J. L. KARDOS, *Polym. Comp.* **15** (1994) 184.
6. Y. B. YANG, J. L. KARDOS, I. S. YOON, S. J. CHOI and M. P. DUDUKOVIC, in Proc. Amer. Soc. Compos., 4th Tech. Conf. (Western Hemisphere Publ., Blacksburg, VA, 1989) p. 36.
7. I. S. YOON, "Experimental Investigation of the Devolatilization in Polyimide Fiber Composites," DSc thesis, Washington University, St. Louis, MO, 1990.
8. I. A. BIESENBERGER and D. H. SEBASTIAN, "Principles of Polymerization Engineering" (John Wiley and Sons, New York, 1983).
9. R. C. REID, J. M. PRAUSNITZ and B. E. POLING, "The Properties of Gases and Liquids," 4th ed. (McGraw Hill, New York, 1987).
10. R. F. SINCOVEC and N. K. MADSEN, *Soft. Nonlin. Part. Differ. Equ.* **1**(3) (1975) 232.
11. "Cambridge Engineering Selector," Version 3.1 (Granta Design Ltd., Cambridge, UK, 2000).

Received 22 January
and accepted 23 June 2003